STRATEGIES FOR MODELLING DELAMINATION GROWTH USING ISOGEOMETRIC CONTINUUM SHELL ELEMENTS

Joris J.C. Remmers[1], Martin Fagerström[2]

[1]Eindhoven University of Technology, Department of Mechanical Engineering
Email: J.J.C.Remmers@tue.nl, Web Page: http://www.tue.nl/mechmat
[2]Chalmers University of Technology, Department of Applied Mechanics
Email: Martin.Fagerstrom@chalmers.se, Web Page:
http://www.chalmers.se/en/departments/am/research/material/Pages/default.aspx

Keywords: Isogeometric Analysis, Delamination, Continuum Shell Formulation, Cohezive zone method

Abstract
The computational efficiency of CAE models and methods for analysing failure progression in composites is important to enable their use in full scale models. In particular, efficient approximation and solution methods for delamination modelling is crucial to meet today's requirements on virtual development lead times. For that purpose, several papers have been published that present alternative methods for modelling concepts which support laminate failure analyses requiring only one shell element through the thickness and where arbitrary delamination propagation is accounted for only in areas where it is needed [1–3]. The proposed new concepts however need to be further developed before they can be readily applied to solve engineering problems. As for the alternative concept based on an isogeometric approach by Hosseini et al.[4], there is a need to handle successive introduction of new discontinuities by means of knot-insertion in an automated fashion. To this end, better predictions of the through-the-thickness distribution of out-of-plane stresses are needed [5]. In this paper we focus on the further development of the isogeometric continuum shell element to allow for an automated insertion of discontinuities.

1. Introduction

Isogeometric analysis (IGA) has recently received much attention in the computational mechanics community. The basic idea is to use splines, which are the functions commonly used in computer-aided design (CAD), as the basis functions for the analysis rather than the traditional Lagrange basis functions [6, 7]. Originally, Non-Uniform Rational B-splines (NURBS) have been used in isogeometric analysis, but their inability to achieve local refinement has driven their gradual replacement by the more advanced T-splines. An important advantage of isogeometric analysis is that the functions used for the representation of the geometry in the CAD drawings are employed directly for the analysis. This avoids the need for a sometimes elaborate meshing procedure. This important feature allows for a design-through-analysis approach, which yields a significant reduction of the time needed for the preparation of the analysis model [7]. Another important advantage is the higher-order continuity of the isogeometric shape functions. This feature allows to calculate higher order derivatives and enables a straightforward implementation of shell theories which require C^1 continuity such as Kirchhoff-Love models [8].

When non-linear material phenomena such as damage or delamination need to be included in the anal-

Excerpt from ISBN 978-3-00-053387-7

ysis, the computation of an accurate three-dimensional stress field in a specific material point in the shell becomes mandatory. In that case, traditional shell elements fall short and continuum shell elements are an obvious alternative, e.g. [9]. An isogeometric version of such a continuum shell element has been presented in [3, 4, 10]. Here, the advantage of an accurate geometric description of the shell mid-surface is combined with the three-dimensional stress representation of conventional continuum shell elements. The formulation adopts NURBS (or T-spline) basis functions for the discretisation of the shell mid-surface, whereas a higher-order B-spline function is used for the interpolation in the thickness direction. An important advantage of using B-spline basis functions is their ability to model weak and strong discontinuities in the displacement field by knot-insertion [11]. Weak discontinuities are usually introduced by subdividing the shell in the thickness direction in multiple layers each having a piecewise polynomial interpolation. Strong discontinuities can be used to model delaminations. Conventionally, these delaminations are modelled using interface elements, or in a more general manner, by exploiting the partition-of-unity property of Lagrange polynomials [1]. The knot-insertion technique allows to do this in an isogeometric analysis formulation in a straightforward manner, as demonstrated by Hosseini *et al.* [3].

In this paper, we extend the isogeometric continuum shell element [3] such that the order of interpolation of the displacement field in the thickness direction is adapted *automatically*. In this way, we can start the analysis with an computationally efficient *lumped* element, which shows a close resemblance to traditional shell elements. When the stress state in the element increase, the basis function in the thickness direction are enhanced by knot-insertion to explicitly model the weak discontinuities at the layer interfaces. Finally, delamination is modelled by another knot-insertion step to arrive at basis functions with strong discontinuities.

This paper is ordered as follows. In the next section, we will give a concise review of the isogeometric continuum shell element, followed by a few numerical examples in Section 3. A strategy to perform the automatic knot-insertion to enhance the interpolation in thickness direction is presented in Section 4. Since the out-of-plane stresses in the thickness direction of the lumped element are of a rather poor quality, an algorithm to reconstruct these stresses [5] is presented as well. The paper is closed with some conclusions and an outlook to future developments.

2. Isogeometric continuum shell element

The kinematic relations and the discretisation of the isogeometric continuum shell element, discussed in this section, are presented in detail in Hosseini *et al.* [3].

2.1. Kinematics and equilibrium equations

Figure 1 shows the undeformed and the deformed configuration of a continuum shell element. The reference surface of the shell is denoted by S^0. The variables ξ and η are the local curvilinear coordinates in the two independent in-plane directions, and ζ is the local curvilinear coordinate in the thickness direction. The position of a material point within the shell body in the undeformed configuration is written as a function of the three curvilinear coordinates:

$$\mathbf{X}(\xi,\eta,\zeta) = \mathbf{X}^0(\xi,\eta) + \zeta\mathbf{D}(\xi,\eta)\ ,\ 0 \le \zeta \le 1 \tag{1}$$

where $\mathbf{X}^0(\xi,\eta)$ is the projection of the point on the reference surface of the shell and $\mathbf{D}(\xi,\eta)$ is the thickness director perpendicular to the surface S_0 at this point.

In any material point, a local reference triad can be established. The covariant base vectors are then obtained as the partial derivatives of the position vectors with respect to the curvilinear coordinates Θ^i =

Excerpt from ISBN 978-3-00-053387-7

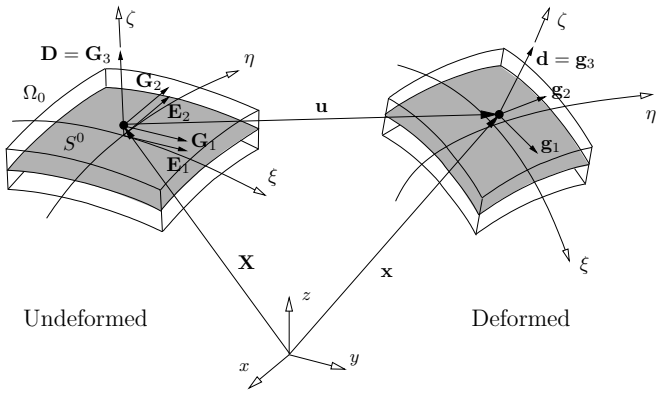

Figure 1. Kinematics of the continuum shell in the undeformed and in the deformed configuration. The corresponding covariant triads for any point in the shell body are denoted by $\mathbf{G}_i$ and $\mathbf{g}_i$.

$[\xi, \eta, \zeta]$. First, we define a set of basis vectors on the reference surface in the undeformed configuration as:

$$\mathbf{E}_\alpha = \frac{\partial \mathbf{X}^0}{\partial \Theta^\alpha} \quad , \quad \alpha = 1, 2 \qquad \text{and} \qquad \mathbf{E}_3 = \mathbf{D} = \frac{\mathbf{E}_1 \times \mathbf{E}_2}{||\mathbf{E}_1 \times \mathbf{E}_2||} t \tag{2}$$

where t is the thickness of the shell. Now, using Equation (1), the covariant triad for any point within the shell body is obtained as:

$$\mathbf{G}_\alpha = \frac{\partial \mathbf{X}}{\partial \Theta^\alpha} = \mathbf{E}_\alpha + \zeta \mathbf{D}_{,\alpha} \quad , \quad \alpha = 1, 2 \qquad \text{and} \qquad \mathbf{G}_3 = \mathbf{D} \tag{3}$$

where the subscript comma denotes partial differentiation.

The position of the material point in the deformed configuration $\mathbf{x}(\xi, \eta, \zeta)$ is related to $\mathbf{X}(\xi, \eta, \zeta)$ via the displacement field $\mathbf{u}(\xi, \eta, \zeta)$ as:

$$\mathbf{x}(\xi, \eta, \zeta) = \mathbf{X}(\xi, \eta, \zeta) + \mathbf{u}(\xi, \eta, \zeta) \tag{4}$$

The displacement field $\mathbf{u}$ can be of any order which is in contrast to the standard continuum shell formulation where an internal stretch term is added to obtain a quadratic term in the displacement field in the thickness direction [9]. The covariant triad at a material point in the deformed configuration $\mathbf{g}_i$ can be calculated in a similar fashion and is used to construct the Green-Lagrange strain tensor. The balance equations are expressed in a Total Lagrange formulation and the resulting system of non-linear equations is typically solved in an incremental - iterative manner. Further details on the derivation of the balance equations and the solution procedure can be found in [3, 4].

2.2. Discretisation

The mid-surface of the shell is constructed using NURBS or T-spline basis functions. The displacement field in the through-the-thickness direction is discretised using higher order B-spline basis functions [4]. In this way, a B-spline volume patch is created by multiplying a bivariate and a univariate spline function. Because of the higher order continuity of the discretisation in thickness direction, the strain field varies at least linearly over the thickness, which is important to avoid thickness locking [9]. The B-spline basis functions that are used to construct the displacement field in the through-the-thickness direction is C^{p-k} continuous at a knot with multiplicity k [12]. This means that we are able to control the continuity of the basis functions at a knot by arbitrarily selecting its multiplicity. This property is useful in modelling traction-free cracks and adhesive interfaces (strong discontinuity) and layered structures with C^0 continuity between the layers (weak discontinuity) [11].

Excerpt from ISBN 978-3-00-053387-7

Figure 2 shows the steps in order to make a discontinuity in the thickness direction of a shell structure. Assume that a quadratic B-spline basis function h_i defined over a knot vector $\mathcal{T} = [0, 0, 0, \frac{1}{2}, 1, 1, 1]$ has been used. This gives us four basis functions which are all C^1 continuous at $\zeta = \frac{1}{2}$. In the remainder, this element will be called the *lumped* element. Now suppose that we want to have a composite shell consisting of two layers of equal thickness. The deformation of composite structures requires a unique displacement at the interfaces and different strain fields in the adjacent layers. In the example of Figure 2 this is simply achieved by having a displacement field which is C^0 continuous at the interface $\zeta = \frac{1}{2}$. This leads to the new knot vector $\mathcal{T} = [0, 0, 0, \frac{1}{2}, \frac{1}{2}, 1, 1, 1]$. Henceforth, we will denote this element as the *layered* element. Subsequently, the complete separation of the layers is obtained if we insert the second knot as: $\mathcal{T} = [0, 0, 0, \frac{1}{2}, \frac{1}{2}, \frac{1}{2}, 1, 1, 1]$, and this element will be denoted as the *discontinuous* element. Figure 2 shows the corresponding basis functions through the knot insertion process.

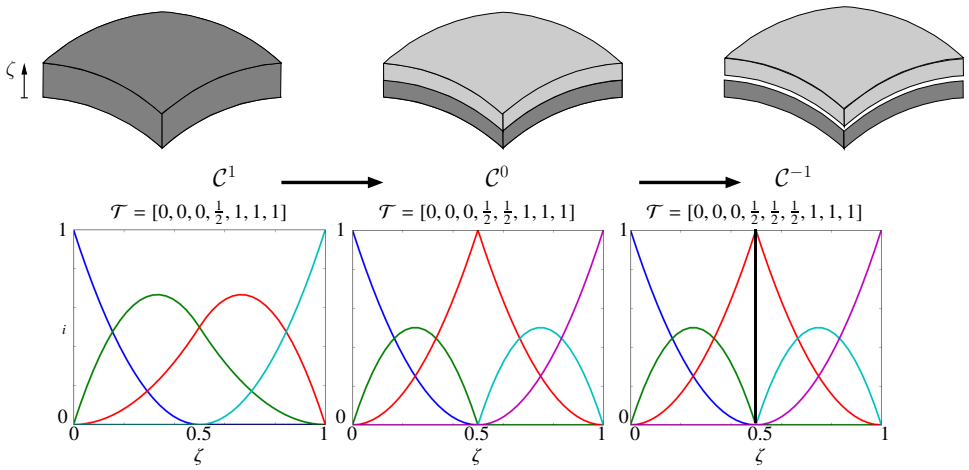

Figure 2. Schematic representation of introducing a discontinuity in the thickness direction of a shell. Weak and strong discontinuities between the layers of a composite shell are created by knot-insertion. In the remainder of this chapter, the three configurations will be denoted by *lumped*, *layered* and *discontinuous* (from left to right).

3. Numerical Examples

The performance of the continuum shell element is first studied in the simulation of the deflection of a multi-layer composite panel. Conventionally, these structures are simulated with a zero-thickness shell element. This is generally sufficient for calculating displacements, but it does not allow for computing the stresses and strains in the individual layers accurately.

We consider the laminate shown in Figure 3 [4]. The panel consists of six layers of a unidirectional material, with a stacking sequence $[0, 90, 0]_s$. Each layer is 0.2 mm thick, so that the total thickness of the shell is 1.2 mm. The layers can be modelled as transversely isotropic. The panel is simply supported on all four sides and is loaded by a distributed out-of-plane load with amplitude $q_0 = 1$ MPa. The panel has been simulated for three different discretisations: second-order in the thickness direction, fourth-order in the thickness direction (denoted as *lumped*(2) and *lumped*(4), respectively, in Figure 2) and second-order per layer with weak discontinuities at the boundaries between the layers (*layered*(2) in Figure 2). A reference solution for the out-of-plane displacement of the mid-point is obtained from classical laminate theory. Figure 4(a) shows σ_{xx} in the mid-point of the panel as a function of the thickness coordinate of the shell obtained for different discretisations. The results from one second-order and one fourth-order B-spline element, lead to the same stress distribution as that of a second-order B-spline per layer (weak discontinuities at layer boundaries). All the results are in agreement with the reference solution from the classical laminated plate theory.

Excerpt from ISBN 978-3-00-053387-7

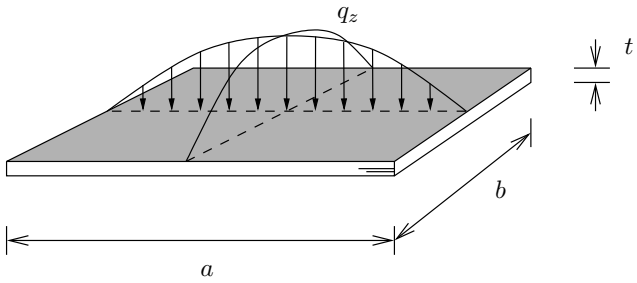

Figure 3. Geometry and loading conditions of a rectangular panel. All four edges are simply supported.

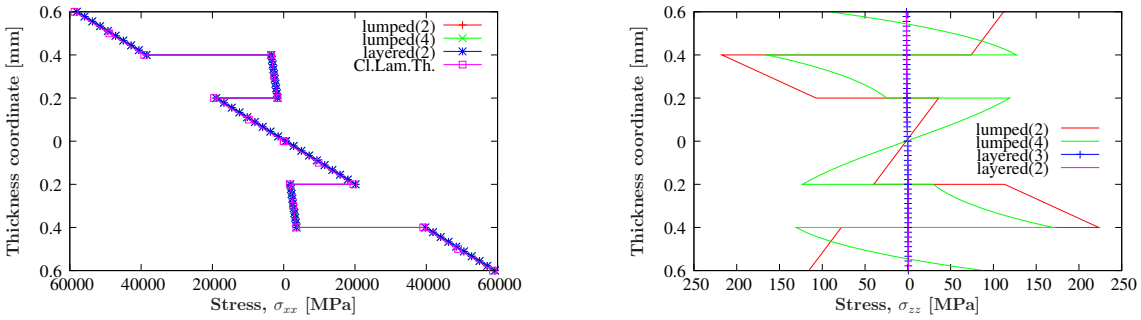

(a) σ_{xx} stress (b) σ_{zz} stress

Figure 4. Stresses at the mid-point as a function of the thickness of the panel for *lumped* and *layered* discretisations with B-splines of various orders in thickness direction. The thickness of the panel is 1.2 mm [4].

Next, the ability of the shell element to compute interlaminar stresses is examined. This issue is of importance when damage and failure of composite materials need to be considered in the simulations. The normal stress σ_{zz} is presented in Figure 4(b) as a function of thickness of the shell. By using second-order and third-order B-splines per layer, the *layered* (2) and *layered* (3) elements, respectively, which are C^0 continuous at the interfaces, we can capture a σ_{zz} distribution in the thickness direction, which is zero through most of the thickness and equals $q_0 = 1$ MPa at the top surface. Adopting just one element of second-order and of fourth-order B-splines, *lumped* (2) and *lumped* (4), respectively, for the discretisation in the thickness direction results in a fluctuation of the σ_{zz} distribution. From these results it is concluded that the *lumped* elements fail to accurately compute σ_{zz} stresses. In order to apply a stress based criterion to upgrade these elements to *layered*, we need to reconstruct these stresses.

In the next example delamination propagation is simulated in a curved panel. The geometry of the panel is shown in Figure 5. The panel is considered to have two isotropic layers with identical elastic properties. An initial delamination is taken over an angle $\frac{\pi}{8}$. The curved panel is clamped at one edge and subjected to a constant distributed load of q_x. This provides a suitable test case to investigate mixed-mode delamination propagation with large rotations at the interface. Delamination growth can be modelled by extending the weak form of the equilibrium conditions with a cohesive zone traction term. The opening of this interface is equal to the relative displacements of two material points on either side of the interface. A detailed description of this term can be found in [3].

Figure 5 shows the deformation of the panel. First, both layers start moving in the loading direction. In this process damage at the interface starts to grow. After a certain deformation and a certain damage growth, the lower layer moves in the reverse direction while the top layer keeps moving in the loading direction. At the final stage, the lower layer has returned to its initial configuration, the interface is fully

Excerpt from ISBN 978-3-00-053387-7

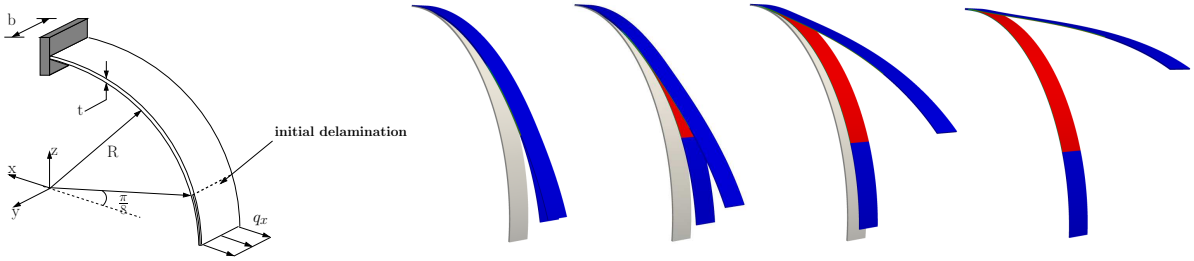

Figure 5. Geometry and deformation of the curved panel with two layers and an initial delamination. Gray indicates the initial configuration, red represents the areas with damage $\omega \approx 1$ and blue shows the areas with $\omega = 0$ [3].

damaged and the upper layer remains in the new configuration.

4. Adaptive discretisation

In the examples in the previous section, the discretisation in the thickness direction is fixed. In principle, the order of the discretisation can be changed during the simulation by means of a stress based criterion. To enable such an automatic update of the discretisation, two essential problems have to be addressed. First in order to enhance the element from *lumped* to *layered*, see Fig. 2, the stress state in the *lumped* element has to be recovered. Second, the initial values of new degrees of freedom of the element needs to be determined .

4.1. Stress enhancement scheme

Transverse out-of-plane stresses evaluated directly from the *lumped* shell element are, as a consequence of the adopted simplified kinematics, generally of poor accuracy. To still be able to obtain reliable predictions of these stresses as input to the update criterion, we adopt a strategy similar to Kant and Manjunatha [13] and Park *et al.* [14] where improved values are recovered from the 3-dimensional momentum balance equations. Thus, we reconstruct the transverse stress variation through the thickness of the shell via thickness integration of these equations. For zero body forces under quasi-static conditions we can find the transverse stresses as:

$$\hat{\sigma}^k_{\alpha 3} = -\sum_{n=1}^{k} \int_{\zeta^{(n-1)}}^{\zeta^{(n)}} (\sigma_{\alpha 1,1} + \sigma_{\alpha 2,2})\, \mathrm{d}\zeta + C_\alpha, \qquad \hat{\sigma}^k_{33} = \sum_{n=1}^{k} \int_{\zeta^{(n-1)}}^{\zeta^{(n)}} \int_{\zeta^{(n-1)}}^{\zeta^{(n)}} (\sigma_{11,11} + \sigma_{22,22} + 2\sigma_{11,12})\, \mathrm{d}\zeta \mathrm{d}\zeta + C_3\zeta + C_4, \quad (5)$$

where ζ is the local transverse direction, $\zeta^{(n-1)}$ and $\zeta^{(n)}$ denote the lower and upper thickness coordinate of ply n, $\bullet_{,i}$ and $\bullet_{,ii}$ denote the first and second derivative with respect to coordinate $i = [1, 2]$ and where $\hat{\bullet}$ denotes recovered values. As can be seen above, the integration of the 3D equilibrium equations yields integration constants which in the general case have to be determined from the traction conditions at the top and bottom shell surface, cf. Främby *et al.* [15]. It is in that paper also shown that the integration constants can be used to average the integration error[1] over the thickness, such that the discrepancy between the predicted stresses at the surfaces and the applied tractions is minimised. In this work, we consider only homogeneous traction boundary conditions at the top and bottom of the shell, whereby we choose to set these constants to zero.

Furthermore, since the integrations in (5) involves the in-plane first and second derivatives of the in-plane stress components, these need to be extracted from the solution. In traditional finite element analyses

[1]Integrating Eq. (5 from the bottom to the top surface often leads to a small resulting shear traction at the top even if the surface is traction free, due to the numerical errors introduced during the procedure.

Excerpt from ISBN 978-3-00-053387-7

with shells, the in-plane stress components are predicted with good accuracy, cf. as demonstrated in Fig. 4(a). However, the stress derivatives are not because of only C^0 in-plane continuity of the shape functions. Since the derivatives of these traditional shape functions are discontinuous across element edges, the resulting stresses are non-smooth also for elastic problems. The benefit from an IGA approach on the other hand is that stresses indeed are smooth when crossing element edges, and that, thereby, the derivatives of each component can be computed element wise with good accuracy.

With the current IGA approach, one way to calculate the stress gradients would be to compute the third gradients of the displacement approximation, and then calculate the stress derivatives directly. However, this requires a displacement approximation of at least order three, which is believed to be too computationally expensive. In addition, the through-the-thickness discontinuity in these gradients would not be well captured with the current *lumped* approximation. Instead, we make use of the stress smoothness and project in each element the stress variation in each plane of integration points on a second order Lagrangian basis (using conventional second order finite element shape functions). This projected stress field can then, for each layer of integration points, be used to evaluate first and second derivatives of each stress component in the element centre point at a given position through the thickness. As final step, we then integrate the stress derivatives according to Equation (5) to obtain the recovered stress profile. As a result, we obtain an accurate prediction of the through-the-thickness variation of the transverse stresses even when a *lumped* thickness discretisation is used.

4.2. Initialisation of new degrees of freedom

When an element is enhanced, the displacement field in a knot is discretised using more degrees of freedom. The initial value of these new degrees of freedom is not equal to zero, in contrast to most X-FEM procedures. Instead, these initial values must be calculated using the values of the existing degrees of freedom (which in turn will obtain other values too).

When the order of an element is changed, the displacement field in the through-the-thickness direction is updated. Assume that before the update, the interpolation in the thickness direction consists of m shape functions. Each knot then supports $3m$ degrees of freedom to construct the x, y and z displacement fields. These nodal degrees of freedom are denoted $\mathbf{a}_j$, where $j = [x, y, z]$. After the update, the number of shape functions has increased and the corresponding nodal degrees of freedom are denoted as $\mathbf{a}^*_j$. The initial values of this new vector can be obtained from the old nodal values using a minimisation procedure:

$$\mathbf{M}\mathbf{a}^*_j = \mathbf{b}_j \qquad \forall \;\; j = [x, y, z] \qquad \text{where} \quad \mathbf{M} = \int_\zeta \mathbf{\Psi}^{*\mathrm{T}}\mathbf{\Psi}^* \mathrm{d}\zeta \quad \text{and} \quad \mathbf{b} = \int_\zeta \mathbf{\Psi}^{*\mathrm{T}}\left(\mathbf{\Psi}\mathbf{a}_j\right)\mathrm{d}\zeta \qquad (6)$$

In this equation $\mathbf{\Psi}$ and $\mathbf{\Psi}^*$ denote the array of basis functions in the through-the-thickness direction before and after the update. Note that this procedure needs to be repeated for the three displacement components in x, y and z direction.

5. Conclusions

In this paper we present an isogeometric continuum shell element in which the interpolation in thickness direction can be modified automatically in order to improve the accuracy of the element under high stress states and to model delamination growth. The use of isogeometric shape functions is essential here. It enables to introduce weak and strong discontinuities by knot insertion. Furthermore, the higher order continuity allows to reconstruct the rather poor stress representation. The application of the approach in large scale analyses however remains to be demonstrated.

Excerpt from ISBN 978-3-00-053387-7

Acknowledgments

The authors acknowledge support from the Swedish strategic innovation programme LIGHTer provided by VINNOVA (grant no. 2014-06041).

References

[1] J.J.C. Remmers, G.N. Wells, and R. de Borst. A solid-like shell element allowing for arbitrary delaminations. *International Journal for Numerical Methods in Engineering*, 58:2013–2040, 2003.

[2] J. Brouzoulis and M. Fagerström. An enriched shell element formulation for efficient modeling of multiple delamination propagation in laminates. *Composite Structures*, 126:196–206, 2015.

[3] S. Hosseini, J.J.C. Remmers, C.V. Verhoosel, and R. de Borst. Propagation of delamination in composite materials with isogeometric continuum shell elements. *International Journal for Numerical Methods in Engineering*, 102(3-4):159–179, 2015.

[4] S. Hosseini, J.J.C. Remmers, C.V. Verhoosel, and R. de Borst. An isogeometric continuum shell element for non-linear analysis. *Computer Methods in Applied Mechanics and Engineering*, 271:1–22, 2014.

[5] J. Främby, J. Brouzoulis, and M. Fagerström. Assessment of two methods for the accurate prediction of transverse stress distributions in laminates. *Composite Structures*, 140:602–611, 2016.

[6] T.J.R. Hughes, J.A. Cottrell, and Y. Bazilevs. Isogeometric analysis: Cad, finite element, nurbs, exact geometry and mesh refinement. *Computer Methods in Applied Mechanics and Engineering*, 194:4135–4195, 2005.

[7] J. Cottrell, T.J.R. Hughes, and Y. Bazilevs. *Isogeometric Analysis: Toward Integration of CAD and FEA*. John Wiley & Sons, Chichester, 2009.

[8] J. Kiendl, K.U. Bletzinger, J. Linhard, and R. Wüchner. Isogeometric shell analysis with kirchhoff-love elements. *Computer Methods in Applied Mechanics and Engineering*, 198:3902–3914, 2009.

[9] H. Parisch. A continuum-based shell theory for non-linear application. *International Journal for Numerical Methods in Engineering*, 38:1855–1883, 1995.

[10] S. Hosseini, J.J.C. Remmers, C.V. Verhoosel, and R. de Borst. An isogeometric solid-like shell formulation for non-linear analysis. *International Journal for Numerical Methods in Engineering*, 95:238–256, 2013.

[11] C.V. Verhoosel, M.A. Scott, R. de Borst, and T.J.R. Hughes. An isogeometric approach to cohesive zone modeling. *International Journal for Numerical Methods in Engineering*, 87(1-5):336–360, 2011.

[12] L. Piegl and W. Tiller. *The NURBS Book, Second Edition*. Springer-Verlag, New York, 1997.

[13] T. Kant and B.S. Manjunatha. On accurate estimation of transverse stresses in multilayer laminates. *Computers & Structures*, 74:351–365, 1994.

[14] B.C Park, J.W Park, and Y.H. Kim. Stress recovery in laminated composite and sandwich panels undergoing finite rotations. *Composite Structures*, 59:227–235, 2003.

[15] J. Främby, M. Fagerström, and J. Brouzoulis. Delamination initiation and propagation modelling in an enriched shell element formulation. In *Proc. 17th European Conference on Composite Materials*, Munich, Germany, 2016.